

# Multiple-LED Complex Modulation Schemes for Indoor MIMO VLC Systems

K. V. S. Sai Sushanth and A. Chockalingam

Department of ECE, Indian Institute of Science, Bangalore 560012

**Abstract**—In this paper, two complex modulation schemes suited for use in multiple-input multiple-output (MIMO) visible light communication (VLC) systems are proposed and their performance investigated. The proposed schemes are quadrature spatial modulation (QSM) and dual mode index modulation (DMIM) with a dual-LED complex modulator (DCM) used as the basic building block (termed as DCM block) to transmit complex modulation symbols. The proposed schemes, referred to as QSM-DCM and DMIM-DCM schemes, do not require Hermitian symmetry operation to transmit complex modulation symbols. The proposed schemes are shown to achieve enhanced rates and good performance in indoor MIMO VLC settings. Compared to spatial modulation DCM (SM-DCM) scheme known in the recent literature, the proposed schemes achieve significantly better performance. Results show that, at a bit error rate of  $10^{-5}$ , performance gains up to 10.2 dB and 7.4 dB can be achieved using the proposed QSM-DCM and DMIM-DCM schemes, respectively. Also, the spatial performance investigation indicates that the proposed schemes outperform the SM-DCM scheme for most of the receiver locations across the room.

**Keywords** – Visible light communication, MIMO VLC, multiple-LED complex modulation, bit error rate, spatial performance.

## I. INTRODUCTION

The radio frequency (RF) spectrum is getting crowded due to rapid adoption of mobile communication devices and services. Wireless communication using millimeter wave frequencies (e.g., 28 to 60 GHz bands with large available bandwidths) is emerging as a popular approach to satisfy the growing demand for wireless capacity. Another promising approach is the use of visible light spectrum for wireless data transmission. Termed as ‘visible light communication’ (VLC), this approach is emerging as an attractive alternative to the RF communication approach [1]. In VLC systems, light emitting diodes (LED) serve as light sources that transmit data wirelessly in visible light wavelengths (400 to 700nm). At the receiver, photo detectors (PD) are used to detect the received signals.

Intensity modulation with direct detection (IM/DD) is widely used in VLC systems, where the LEDs are intensity modulated to transmit data and the PDs detect the received intensities. Since information is conveyed by varying the light intensity, real and non-negative signals are used to modulate LEDs in VLC. The use of multiple LEDs and multiple PDs in multiple-input multiple-output (MIMO) configuration is an attractive way to increase spectral efficiency in VLC systems.

This work was supported in part by J. C. Bose National Fellowship, Department of Science and Technology, Government of India, and the Intel India Faculty Excellence Program.

Complex signal sets such as  $M$ -ary quadrature amplitude modulation (QAM) are often used in OFDM based indoor VLC systems. In [2]-[4], several variants of OFDM for VLC have been reported. Some of the schemes reported in these works include dc-biased optical (DCO) OFDM, asymmetrically clipped optical (ACO) OFDM, flip OFDM, non-dc biased (NDC) optical OFDM, and index modulation for NDC-OFDM. A key constraint in all these schemes is the need for Hermitian symmetry operation that converts the complex symbols to real non-negative signals, which compromises the transmission rate in the process. Multiple-LED complex modulation schemes that can eliminate the use of Hermitian symmetry operation have been reported in the recent literature. These schemes include quad-LED complex modulation (QCM) and dual-LED complex modulation (DCM) [5]. The QCM and DCM schemes have been shown to achieve good performance compared to other MIMO modulation schemes such as SMP, SM, GSM [5].

In this paper, considering DCM complex modulator as the elementary building block, we devise two new MIMO VLC modulation schemes. These schemes are inspired by RF index modulation schemes proposed recently, namely, quadrature spatial modulation (QSM) and dual mode index modulation (DMIM) [6],[7]. We term the proposed schemes as QSM-DCM and DMIM-DCM, respectively. In the proposed schemes, the LEDs are partitioned into multiple DCM blocks and signaling is done using these DCM blocks. The proposed schemes achieve enhanced rates and the proposed signaling designs for LED compatible VLC transmission in these schemes are novel. We evaluate the bit error performance of the proposed schemes in indoor VLC settings using analysis and simulations. We compare the performance achieved in these schemes with that of the spatial modulation DCM (SM-DCM) scheme reported in the literature [5]. Our results show that, at a bit error rate (BER) of  $10^{-5}$ , the proposed QSM-DCM and DMIM-DCM schemes can achieve performance gains up to 10.2 dB and 7.4 dB, respectively, compared to the SM-DCM scheme. We also compute the spatial distribution of best performing modulation scheme among QSM-DCM, DMIM-DCM, and SM-DCM, based on a normalized minimum Euclidean distance metric. Results show that the proposed modulation schemes outperform SM-DCM scheme for most of the receiver locations across the room.

## II. INDOOR MIMO VLC SYSTEM MODEL

Consider an indoor MIMO VLC system where the transmitter consists of  $N_t$  LEDs, and the receiver consists of  $N_r$

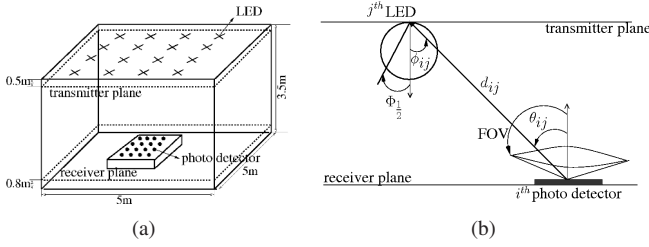


Fig. 1. (a) Geometric setup of a typical indoor MIMO VLC system. (b) LOS channel between  $j$ th LED and  $i$ th PD.

PDs as shown in Fig. 1(a). A room of size  $5\text{m} \times 5\text{m} \times 3.5\text{m}$  is considered. The LEDs are placed in the transmitter plane which is  $0.5\text{m}$  below the ceiling. The PDs are placed on a table located at  $0.8\text{m}$  above the ground. At the transmitter, LEDs convert the data stream in the electrical domain to optical domain. Assume that each LED emits unpolarized white light with Lambertian radiation pattern. Based on the MIMO modulation scheme used, each LED emits light with certain intensity in a given channel use. The transmit signal vector  $\mathbf{x}$  of dimension  $N_t \times 1$  is  $\mathbf{x} = [x_1 \ x_2 \ \dots \ x_{N_t}]^T$ , where  $x_j$  denotes the light intensity emitted by the  $j$ th LED. At the receiver,  $N_r$  PDs convert the received signals from optical to electrical domain and detect the transmitted data. The line-of-sight (LOS) channel gain between the  $j$ th LED and  $i$ th PD, denoted by  $h_{ij}$ , can be calculated as (Fig. 1(b)):

$$h_{ij} = \frac{m+1}{2\pi} \cos^m \phi_{ij} \cos \theta_{ij} \frac{A}{d_{ij}^2} \text{rect}\left(\frac{\theta_{ij}}{FOV}\right), \quad (1)$$

where  $m$  is the mode number of the radiating lobe given by  $m = \frac{-\ln(2)}{\ln \cos \Phi_{\frac{1}{2}}}$ ,  $\Phi_{\frac{1}{2}}$  is the half-power semi-angle of the LEDs,  $A$  is the area of the PD, FOV is the field-of-view of the PD, and  $\text{rect}(z) = 1$ , if  $|z| \leq 1$ , and  $\text{rect}(z) = 0$ , if  $|z| > 1$ ,  $d_{ij}$  is the LOS distance between  $j$ th LED and  $i$ th PD,  $\phi_{ij}$  is the angle of emergence for  $j$ th LED with respect to its normal, and  $\theta_{ij}$  is the angle of incidence at the  $i$ th PD. The  $N_r \times N_t$  MIMO channel matrix  $\mathbf{H}$  is given by  $[h_{ij}]$ , ( $1 \leq i \leq N_r, 1 \leq j \leq N_t$ ).

The received signal vector of dimension  $N_r \times 1$  (in the electrical domain) at the receiver is given by

$$\mathbf{y} = a\mathbf{H}\mathbf{x} + \mathbf{n}, \quad (2)$$

where  $\mathbf{n}$  is the noise vector of dimension  $N_r \times 1$ ,  $a$  is the responsivity of the PD (in Amp/Watt), and  $\mathbf{x}$  is the transmit signal vector. The elements of transmit signal vector  $\mathbf{x}$  are optical intensity values which are determined based on the modulation scheme used. Each element in the noise vector  $\mathbf{n}$  is the sum of received thermal noise and ambient light noise, and can be modeled as i.i.d. real AWGN with zero mean and variance  $\sigma^2$ . The average received SNR in the electrical domain is given by  $\bar{\gamma} = \frac{a^2}{\sigma^2 N_r} \sum_{i=1}^{N_r} \mathbb{E}\{(\mathbf{H}_i \mathbf{x})^2\}$ .

#### A. Normalized minimum Euclidean distance metric

For a given  $\mathbf{H}$ , let  $\mathbb{S}_{\text{Rx}} = \{\mathbf{H}\mathbf{x}_1, \mathbf{H}\mathbf{x}_2, \dots, \mathbf{H}\mathbf{x}_L\}$  denote the received signal set corresponding to the transmit signal set  $\mathbb{S}_{\text{Tx}}$ , in the absence of noise. The set of normalized received signal vectors (i.e., vectors in  $\mathbb{S}_{\text{Rx}}$  normalized by the average received signal power) is given by  $\tilde{\mathbb{S}}_{\text{Rx}} = \{\tilde{\mathbf{y}}_1, \tilde{\mathbf{y}}_2, \dots, \tilde{\mathbf{y}}_L\}$ , where  $\tilde{\mathbf{y}}_i =$

$\frac{\mathbf{H}\mathbf{x}_i}{\sqrt{\frac{1}{LN_r} \sum_{i=1}^L \|\mathbf{H}\mathbf{x}_i\|^2}}$ . The minimum Euclidean distance of the normalized received signal set is

$$\tilde{d}_{\min, \mathbf{H}} = \min_{\tilde{\mathbf{y}}_i, \tilde{\mathbf{y}}_j \in \tilde{\mathbb{S}}_{\text{Rx}}, i \neq j} \|\tilde{\mathbf{y}}_i - \tilde{\mathbf{y}}_j\|. \quad (3)$$

Let  $\mathbb{S}_{\text{Tx}}^{(1)}$  and  $\mathbb{S}_{\text{Tx}}^{(2)}$  denote the signal sets of two different modulation schemes, and let  $\tilde{d}_{\min, \mathbf{H}}^{(1)}$  and  $\tilde{d}_{\min, \mathbf{H}}^{(2)}$  denote their corresponding normalized minimum Euclidean distances, for a given  $\mathbf{H}$ . In the high SNR regime, the BER performance of modulation scheme with signal set  $\mathbb{S}_{\text{Tx}}^{(1)}$  will be better than that of the scheme with  $\mathbb{S}_{\text{Tx}}^{(2)}$ , if  $\tilde{d}_{\min, \mathbf{H}}^{(1)} > \tilde{d}_{\min, \mathbf{H}}^{(2)}$ . Also, the SNR gap between the BER performance of the two modulation schemes in the high SNR regime is given by  $20 \log(\tilde{d}_{\min, \mathbf{H}}^{(1)} / \tilde{d}_{\min, \mathbf{H}}^{(2)})$ .

#### B. DCM scheme

The proposed modulation schemes (presented in the next section) are based on the DCM scheme in [5]. Here, we briefly introduce the DCM scheme. DCM scheme exploits the polar representation of complex numbers to implement a complex modulator unit suited for VLC. A DCM transmitter consists of two LEDs. One LED conveys the magnitude and the other LED conveys the phase of a complex symbol. The complex modulation symbol  $s$  can be written in the form

$$s = r e^{j\phi}, \quad (4)$$

where  $r = |s|$ ,  $r \in \mathbb{R}^+$ , and  $\phi = \angle s$ ,  $\phi \in [0, 2\pi)$ . One LED emits intensity  $r$  and the other LED emits intensity  $\phi$ . That is, the transmit vector  $\mathbf{x}$  is a  $2 \times 1$  vector given by  $\mathbf{x} = [r \ \phi]^T$ . The advantages of DCM are simplicity and good performance [5]. In the next section, we present the proposed multiple-LED modulation schemes where the LEDs at the transmitter are grouped as multiple DCM blocks and signaling is done using these DCM blocks.

### III. PROPOSED MODULATION SCHEMES

In this section, we introduce the proposed QSM-DCM and DMIM-DCM schemes with DCM as the basic building block.

#### A. Proposed QSM-DCM scheme

The QSM-DCM scheme uses  $N_t$  LEDs, where  $N_t = 2^k$  and  $k$  is an integer  $\geq 2$ . The  $N_t$  LEDs are grouped into  $N_p = \frac{N_t}{2}$  DCM blocks, each with two LEDs. The number of bits conveyed in one channel use in QSM-DCM is  $2 \log_2 N_p + \log_2 M$ , where  $M$  is the size of a complex modulation alphabet (denoted by  $\mathbb{A}$ ) such as QAM/PSK, i.e.,  $M = |\mathbb{A}|$ . Here,  $2 \log_2 N_p$  bits are used to index the DCM blocks, and  $\log_2 M$  bits are mapped to an  $M$ -ary modulation symbol from  $\mathbb{A}$ . Figure 2 shows the block diagram of a QSM-DCM transmitter for the case with  $N_t = 4$  and  $N_p = 2$  (i.e., there are two DCM blocks identified as DCM Block 1 and DCM Block 2). The signaling architecture proposed to convey  $2 \log_2 2 + \log_2 M = 2 + \log_2 M$  bits in a channel use is as follows.

Let  $b_1$  and  $b_2$  denote the two index bits. The  $(b_1, b_2)$  combination decides what get transmitted by DCM Block 1 (formed by LEDs 1 and 2) and DCM Block 2 (formed by LEDs 3 and 4). Let  $s \in \mathbb{A}$  denote the  $M$ -ary complex

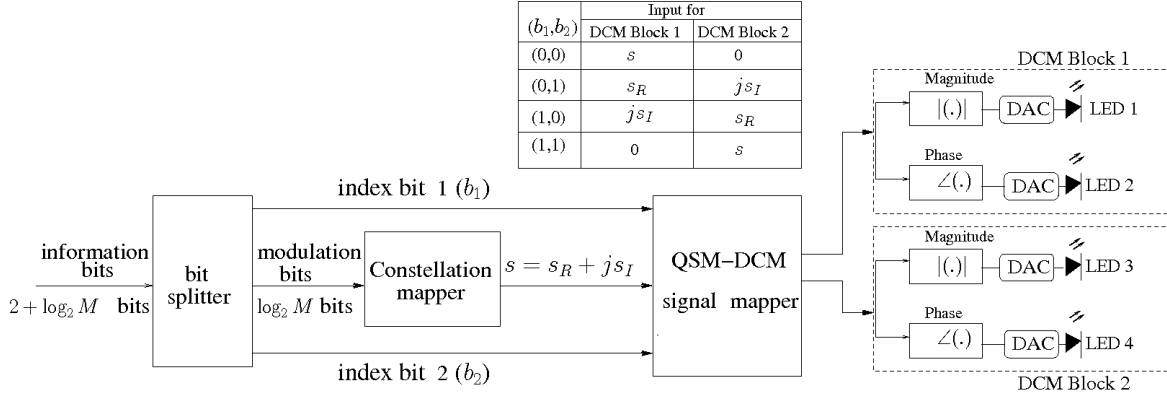


Fig. 2. Proposed QSM-DCM transmitter  $N_t = 4$  and  $N_p = 2$ .

modulation symbol, and let  $s_R$  and  $s_I$  denote the real and imaginary parts of  $s$ , respectively, i.e.,  $s = s_R + js_I$ .

- If  $(b_1, b_2) = (0, 0)$ , then DCM Block 1 transmits  $s$ , i.e., LED 1 emits with intensity  $|s|$  and LED 2 emits with intensity  $\angle s$ , and DCM Block 2 is inactive. An inactive DCM block can be viewed as transmitting value zero, i.e., both LEDs 3 and 4 emit intensity zero.
- If  $(b_1, b_2) = (0, 1)$ , then DCM Block 1 transmits  $s_R$  and DCM Block 2 transmits  $js_I$ . That is, LEDs 1 and 2 in DCM Block 1 emit intensities  $|s_R|$  and  $\angle s_R$ , respectively. Likewise, LEDs 3 and 4 in DCM Block 2 emit intensities  $|js_I|$  and  $\angle js_I$ , respectively.
- Likewise, if  $(b_1, b_2) = (1, 0)$ , then DCM Block 1 transmits  $js_I$  and DCM Block 2 transmits  $s_R$ .
- Finally, if  $(b_1, b_2) = (1, 1)$ , then DCM Block 1 is inactive and DCM Block 2 transmits  $s$ .

*Example 1:* Consider a QSM-DCM transmitter with two DCM blocks and 4-QAM as the modulation alphabet, i.e.,  $N_p = 2$  and  $M = 4$ . The achieved rate in this system is 4 bpcu. Let the information bits to be sent in a given channel use be 1101. The first two bits (i.e., 11) are mapped to the 4-QAM symbol  $s = 1 - j$ . The remaining two bits (i.e., 01) are index bits which result in the emission of intensities of LEDs 1 to 4 as follows: in the DCM Block 1, LED 1 emits intensity 1 (since  $|s_R| = 1$ ) and LED 2 emits intensity 0, whereas LED 3 and LED 4 emit with intensities 1 (since  $|-j| = 1$ ) and  $3\pi/2$  (since  $\angle -j = 3\pi/2$ ), respectively. Hence, the  $4 \times 1$  transmit vector for this example is  $\mathbf{x} = [1 \ 0 \ 1 \ 3\pi/2]^T$ .

*Note 1:* The QSM-DCM scheme described above for  $N_t = 2^2 = 4$  can be generalized for  $N_t = 2^q$ , where  $q$  is an integer  $> 2$ , in which case signaling is done as follows.  $2 \log_2 N_p$  index bits are partitioned into two sets of index bits, set-1 and set-2, each with  $\log_2 N_p$  index bits. Set-1 index bits are used to select a DCM block among  $N_p$  DCM blocks. Likewise set-2 index bits are used to select a DCM block among  $N_p$  DCM blocks. If set-1 and set-2 index bits are the same, then the same DCM block will be selected by both set-1 and set-2 index bits. In this case,  $s = s_R + js_I$  is sent from that selected DCM block. If set-1 and set-2 index bits are different, then two different DCM blocks will be selected. In this case,  $s_R$  will be sent from the DCM block selected using set-1 index

bits, and  $js_I$  will be sent from the DCM block selected using set-2 index bits.

### B. Proposed DMIM-DCM scheme

The DMIM-DCM scheme also consists of  $N_t$  (even) LEDs forming  $N_p = \frac{N_t}{2}$  DCM blocks. Unlike QSM-DCM which use one complex alphabet, DMIM-DCM uses two complex modulation alphabets, denoted by  $\mathbb{M}_A$  and  $\mathbb{M}_B$ . In each channel use, every DCM block transmits a complex symbol. Out of the  $N_p$  DCM blocks,  $N_a$  DCM blocks (called ‘group-A’ DCM blocks) transmit symbols chosen from alphabet  $\mathbb{M}_A$  and the remaining  $N_p - N_a$  DCM blocks (called ‘group-B’ DCM blocks) transmit symbols chosen from alphabet  $\mathbb{M}_B$ . Out of the  $\binom{N_p}{N_a}$  possible patterns of selecting  $N_a$  group-A DCM blocks from  $N_p$  DCM blocks,  $2^{\lfloor \log_2 \binom{N_p}{N_a} \rfloor}$  patterns are used. So  $\lfloor \log_2 \binom{N_p}{N_a} \rfloor$  bits are used as index bits to determine the indices of the  $N_a$  group-A DCM blocks.

The signal transmission in a given channel use is done as follows. Let  $M_A = |\mathbb{M}_A|$  and  $M_B = |\mathbb{M}_B|$ . Form symbols  $s_1^{(A)}, s_2^{(A)}, \dots, s_{N_a}^{(A)} \in \mathbb{M}_A$  based on  $N_a \log_2 M_A$  bits and transmit these symbols through group-A DCM blocks. Likewise, form symbols  $s_1^{(B)}, s_2^{(B)}, \dots, s_{N_p - N_a}^{(B)} \in \mathbb{M}_B$  based on  $(N_p - N_a) \log_2 M_B$  bits and transmit these symbols through group-B DCM blocks. The achieved rate in DMIM-DCM, therefore, is given by  $\lfloor \log_2 \binom{N_p}{N_a} \rfloor + N_a \log_2 M_A + (N_p - N_a) \log_2 M_B$  bpcu. The alphabets  $\mathbb{M}_A$  and  $\mathbb{M}_B$  are chosen to be disjoint (i.e.,  $\mathbb{M}_A \cap \mathbb{M}_B = \phi$ ) in order to distinguish the symbols from the two alphabets. Figure 3 shows the DMIM-DCM transmitter for  $N_t = 8$  and  $N_p = 4$ . In this system, the number of index bits is 2. Let  $(b_1, b_2)$  denote these two index bits. The index bits to grouping of DCM blocks into group-A and group-B is done as follows.

- If  $(b_1, b_2) = (0, 0)$ , then (A,A,B,B) is the grouping pattern of DCM blocks, i.e., DCM Blocks 1 and 2 form group-A, and DCM Blocks 3 and 4 form group-B.
- If  $(b_1, b_2) = (0, 1)$ , then (B,A,A,B) is the grouping pattern of DCM blocks, i.e., group-A consists of DCM Blocks 2 and 3, and group-B consists of DCM Blocks 1 and 4.
- If  $(b_1, b_2) = (1, 0)$ , then (B,B,A,A) is the DCM blocks grouping pattern.

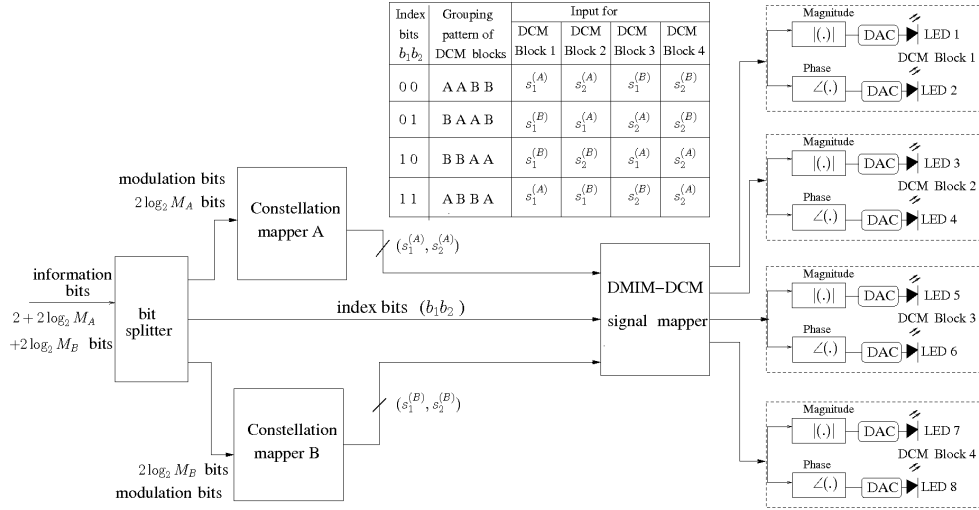


Fig. 3. Proposed DMIM-DCM transmitter with  $N_t = 8$  and  $N_p = 4$ .

- If  $(b_1, b_2) = (1, 1)$ , then (A,B,B,A) is the DCM blocks grouping pattern.

The above signaling scheme can be extended for any even  $N_t$ .

*Example 2:* Consider a DMIM-DCM transmitter with  $N_p = 4$  and  $N_a = 2$ . Let  $\mathbb{M}_A$  and  $\mathbb{M}_B$  be 4-QAM and BPSK, respectively. So the achieved rate is 8 bpcu. There are  $\binom{4}{2} = 6$  patterns of selecting two group-A DCM blocks, and  $2^{\lfloor \log_2 \binom{4}{2} \rfloor} = 4$  patterns among them are chosen. Let (A,A,B,B), (B,A,A,B), (B,B,A,A), and (A,B,B,A) the four chosen patterns (as shown in Fig. 3). Let the information bits to be sent in a channel use be 10110110. The first two bits (10) are the index bits and so (B,B,A,A) is the corresponding DCM blocks grouping pattern (i.e., DCM Blocks 3 and 4 form group-A DCM blocks and DCM blocks 1 and 2 form group-B DCM blocks). The next two pairs of bits (i.e., 11 and 01) select symbols  $s_1^{(A)} = 1 - j$  and  $s_2^{(A)} = -1 - j$ , respectively, from 4-QAM. The last two bits (i.e., 1 and 0) select symbols  $s_1^{(B)} = 1$  and  $s_2^{(B)} = -1$ , respectively, from BPSK. So, DCM Blocks 1, 2, 3, and 4 transmit symbols 1,  $-1$ ,  $1 - j$ ,  $-1 - j$ , respectively. Therefore, the DMIM-DCM  $8 \times 1$  transmit vector for this example is  $\mathbf{x} = [1 \ 0 \ 1 \ \pi \ \sqrt{2} \ 7\pi/4 \ \sqrt{2} \ 5\pi/4]^T$ .

#### IV. PERFORMANCE RESULTS AND DISCUSSIONS

In this section, we present the BER and spatial performance results of the proposed QSM-DCM and DMIM-DCM schemes for two different configurations of indoor MIMO VLC systems, viz.,  $4 \times 4$  and  $8 \times 8$  MIMO configurations. We also compare the performance of the proposed schemes with that of the SM-DCM scheme in [5]. The position of LEDs and PDs for the  $4 \times 4$  and  $8 \times 8$  MIMO configurations are shown in Fig. 4 and Fig. 5, respectively. The system parameters used in the simulation are shown in Table I. In the  $4 \times 4$  system, the four LEDs are paired into two DCM blocks (Block 1 and Block 2 as shown in Fig. 4). In the  $8 \times 8$  system, the eight LEDs are paired into four DCM blocks (Block 1, Block 2, Block 3, and Block 4 as shown in Fig. 5). The complex modulation alphabets used in the considered schemes to achieve rates of

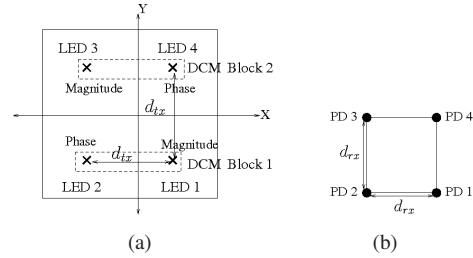


Fig. 4.  $4 \times 4$  indoor MIMO VLC system. (a) Transmitter. (b) Receiver.

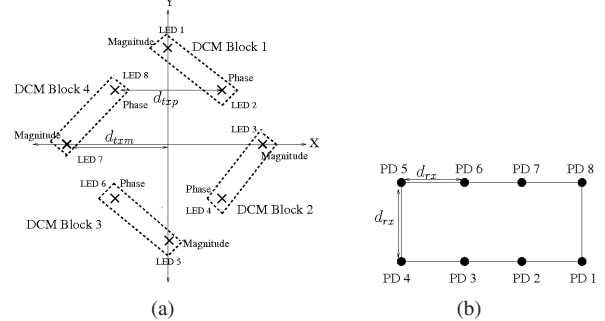


Fig. 5.  $8 \times 8$  indoor MIMO VLC system. (a) Transmitter. (b) Receiver.

4, 6, 8, and 10 bpcu in  $4 \times 4$  and  $8 \times 8$  systems are shown in Tables II and III, respectively. Maximum likelihood detection is used at the receiver.

##### A. BER vs SNR performance of the proposed schemes

In this subsection, we present the BER performance of the proposed schemes obtained through simulation and the analytical upper bound on BER (obtained using union bounding). The receiver is located at the center of the room on the receiver plane (table), i.e., at the coordinate (0m, 0m, 0.8m).

Figures 6(a) and 6(b) show the BER versus SNR plots for QSM-DCM and DMIM-DCM, respectively, in a  $4 \times 4$  MIMO system with 4 bpcu, 6 bpcu, and 8 bpcu. From these figures, it is observed that the analytical upper bounds on BER are very tight in the moderate to high SNR regime. Also, as expected, the use of higher order modulation to achieve

Room	(Length,Width,Height)	(5m,5m,3.5m)
LED	Mode number ( $m$ )	1
	Height from the floor	3m
PD	Responsivity of PD ( $a$ )	0.4 Ampere/Watt
	Field-of-view (FOV)	$85^\circ$
	Height from the floor	0.8m
$4 \times 4$ Transmitter	No. of LEDs ( $N_t$ )	4
	$d_{tx}$	3m
$4 \times 4$ Receiver	No. of PDs	4
	$d_{rx}$	0.1m
$8 \times 8$ Transmitter	No. of LEDs ( $N_t$ )	8
	$d_{txm}$	1.5m
	$d_{txp}$	1.5m
$8 \times 8$ Receiver	No. of PDs	8
	$d_{rx}$	0.1m

TABLE I

SYSTEM PARAMETERS FOR DIFFERENT CONFIGURATIONS OF INDOOR MIMO VLC SYSTEM.

Modulation scheme	$4 \times 4$ MIMO system			
	4 bpcu	6 bpcu	8 bpcu	
QSM-DCM	4-QAM	16-QAM	64-QAM	
DMIM-DCM	$\mathbb{M}_A$	4-QAM	8-QAM	32-QAM
	$\mathbb{M}_B$	BPSK	QPSK	QPSK
SM-DCM	8-QAM	32-QAM	128-QAM	

TABLE II

COMPLEX MODULATION ALPHABETS USED IN VARIOUS SCHEMES FOR DIFFERENT ACHIEVED RATES IN  $4 \times 4$  MIMO VLC SYSTEM.

higher bpcu requires higher SNRs to achieve a certain BER. For example, QSM-DCM requires about 44 dB, 52 dB, and 60 dB to achieve a BER of  $10^{-5}$  for 4-QAM (4 bpcu), 16-QAM (6 bpcu), and 64-QAM (8 bpcu), respectively. These relative performance differences between systems with different bpcu values at high SNRs are found to corroborate with the  $\tilde{d}_{\min, \mathbf{H}}$  based analytical performance prediction. The  $\tilde{d}_{\min, \mathbf{H}}$  values computed for various modulation schemes for different MIMO configurations and bpcu values are presented in Table IV. We can see that the  $\tilde{d}_{\min, \mathbf{H}}$  values for  $4 \times 4$  QSM-DCM for 4 bpcu and 6 bpcu are 0.0470 and 0.0191, respectively. This indicates relatively poor performance for 6 bpcu since the  $\tilde{d}_{\min, \mathbf{H}}$  value for 6 bpcu is smaller than that for 4 bpcu.

Next, we present a comparison between the the BER versus SNR performance achieved by the proposed schemes and the SM-DCM scheme in [5] in a  $8 \times 8$  system. Figures 7(a) and 7(b) show such a comparison for 8 bpcu and 10 bpcu, respectively. It is observed that, in case of 8 bpcu, at  $10^{-5}$  BER, QSM-DCM outperform SM-DCM scheme by 6.65 dB, and DMIM-DCM performs poor among all the three schemes. For the system with 10 bpcu, compared to SM-DCM scheme, performance gains up to 10.25 dB and 7.4 dB are achieved with QSM-DCM and DMIM-DCM, respectively. This can also be verified with from  $\tilde{d}_{\min, \mathbf{H}}$  values of the modulation schemes presented in Table IV. Hence, we observe that at higher bpcu, the proposed QSM-DCM and DMIM-DCM schemes outperform the SM-DCM scheme.

The reason for the superior performance of the proposed schemes compared to that of SM-DCM can be explained as follows. In order to increase the achieved rate, the SM-DCM scheme requires modulation alphabets of larger size when compared to the proposed modulation schemes (see Table II and Table III). Also, the  $\tilde{d}_{\min, \mathbf{H}}$  of a modulation scheme is

Modulation scheme	$8 \times 8$ MIMO system			
	6 bpcu	8 bpcu	10 bpcu	
QSM-DCM	4-QAM	16-QAM	64-QAM	
DMIM-DCM	$\mathbb{M}_A$	BPSK	4-QAM	8-QAM
	$\mathbb{M}_B$	BPSK ( $90^\circ$ rotated)	BPSK	BPSK
SM-DCM	16-QAM	64-QAM	256-QAM	

TABLE III

COMPLEX MODULATION ALPHABETS USED IN VARIOUS SCHEMES FOR DIFFERENT ACHIEVED RATES IN  $8 \times 8$  MIMO VLC SYSTEM.

System	Achieved Rate	$\tilde{d}_{\min, \mathbf{H}}$		
		QSM-DCM	DMIM-DCM	SM-DCM
$4 \times 4$ MIMO	4 bpcu	0.0470	0.0215	0.0505
	6 bpcu	0.0191	0.0128	0.0123
	8 bpcu	0.0061	0.0073	0.0038
$8 \times 8$ MIMO	6 bpcu	0.0278	0.0030	0.0631
	8 bpcu	0.0141	0.0056	0.0070
	10 bpcu	0.0054	0.0051	0.0016

TABLE IV

$\tilde{d}_{\min, \mathbf{H}}$  VALUES FOR QSM-DCM, SM-DCM, AND DMIM-DCM SCHEMES FOR DIFFERENT ACHIEVED RATES IN  $4 \times 4$  AND  $8 \times 8$  MIMO CONFIGURATIONS.

affected by the size of the modulation alphabet used. Hence, in the high SNR regime, at higher bpcu, the performance of SM-DCM scheme degrades more compared to the two proposed schemes, and as a result, SM-DCM scheme achieves relatively poor performance.

### B. Spatial distribution of best performing scheme

As discussed in Sec. II, at high SNR values, the BER performance of a modulation scheme depends on its  $\tilde{d}_{\min, \mathbf{H}}$  value. Specifically, in the high SNR regime, the modulation scheme with a higher  $\tilde{d}_{\min, \mathbf{H}}$  value has better BER performance compared to a modulation scheme having a lower  $\tilde{d}_{\min, \mathbf{H}}$  value. In this subsection, we present the spatial distribution of best performing MIMO modulation scheme among QSM-DCM, DMIM-DCM, and SM-DCM in the high SNR regime. The receiver plane (located at 0.8m above the floor) is divided into a grid of  $200 \times 200$  points and each grid point is considered as a receiver location. At a given receiver location, we obtain the channel gain matrix using (1), and then compute  $\tilde{d}_{\min, \mathbf{H}}$  values using (3), for all the modulation schemes considered. The modulation scheme that has the maximum  $\tilde{d}_{\min, \mathbf{H}}$  value is considered as the best performing modulation scheme for that location. This process is repeated for all the receiver locations across the room. To obtain the spatial distribution plot, each modulation scheme is assigned a particular color (e.g., QSM-DCM: green, DMIM-DCM: black, SM-DCM: blue). Each grid point in the spatial distribution plot is filled with the color of the best performing modulation scheme for that receiver location. From the spatial distribution plots, for each modulation scheme, we also calculated the percentage of the receiver locations at which the modulation scheme considered performed best and presented them in the form of a pie-chart. The spatial distribution plots of the best performing scheme obtained in the case of  $4 \times 4$  system with 6 bpcu and 8 bpcu are shown in Fig. 8. For both 6 bpcu and 8 bpcu, DMIM-DCM is the most favorable scheme across the room as it performs best over 48% and 73% of room area, respectively. In case

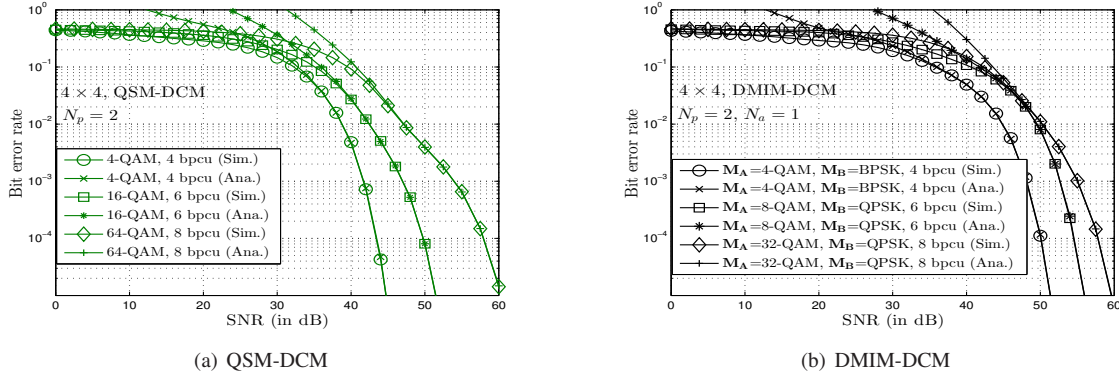


Fig. 6. BER vs SNR performance of the proposed QSM-DCM and DMIM-DCM schemes in  $4 \times 4$  MIMO VLC system with  $N_p = 2$ .

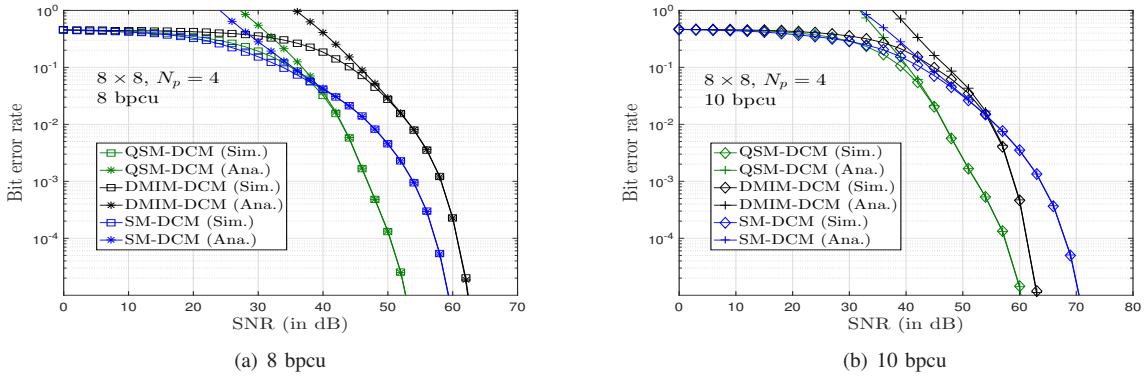


Fig. 7. BER vs SNR performance comparison of proposed modulation schemes with SM-DCM scheme in  $8 \times 8$  MIMO VLC system with  $N_p = 4$ .

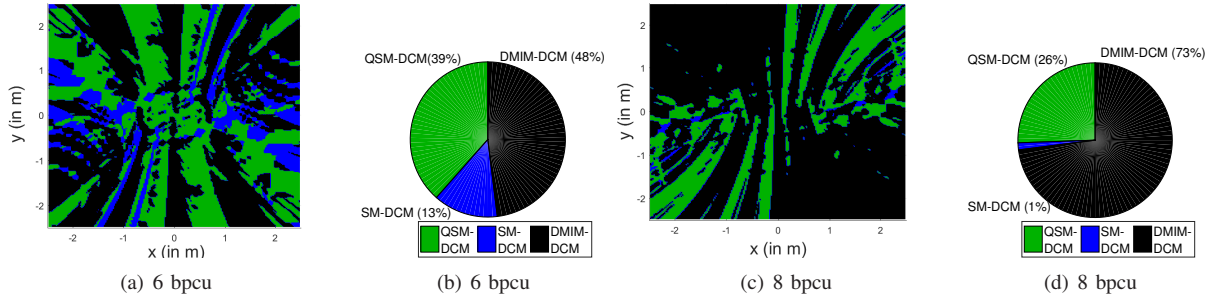


Fig. 8. Spatial distribution of best performing MIMO modulation among QSM-DCM, DMIM-DCM and SM-DCM in  $4 \times 4$  system with 6 bpcu and 8 bpcu.

of 6 bpcu, QSM-DCM and SM-DCM perform best over 39% and 13% area, respectively. In case of 8 bpcu, QSM-DCM and SM-DCM perform best over 26% and 1% area, respectively.

## V. CONCLUSIONS

We proposed efficient multiple-LED modulation schemes that used dual-LED complex modulator (DCM) blocks as the basic building blocks. The proposed schemes, termed as QSM-DCM and DMIM-DCM schemes, are shown to exhibit good distance properties and bit error performance in indoor VLC settings. The spatial distribution of the best performing scheme indicated that one among the two proposed schemes is the best performing scheme in most of the receiver locations across the room. This is because the proposed schemes could use small-sized complex modulation alphabets for a given achieved rate.

## REFERENCES

- [1] D. O'Brien, "Visible light communications: challenges and possibilities," *Proc. IEEE PIMRC 2008*, Sep. 2008.
- [2] J. Armstrong and B. J. Schmidt, "Comparison of asymmetrically clipped optical OFDM and DC-biased optical OFDM in AWGN," *IEEE Commun. Lett.*, vol. 12, no. 5, pp. 343-345, May 2008.
- [3] N. Fernando, Y. Hong, and E. Viterbo, "Flip-OFDM for optical wireless communications," *Proc. IEEE ITW 2011*, pp. 5-9, Oct. 2011.
- [4] S. P. Alaka, T. Lakshmi Narasimhan, and A. Chockalingam, "Coded index modulation for non-DC-biased OFDM in multiple LED visible light communication," *Proc. IEEE VTC 2016-Spring*, May 2016.
- [5] T. Lakshmi Narasimhan, R. Tejaswi, and A. Chockalingam, "Quad-LED and dual-LED complex modulation for visible light communication," online: arXiv: 1510.08805v3 [cs.IT] 24 Jul 2016.
- [6] R. Mesleh, S. S. Ikki, and H. M. Aggoune, "Quadrature spatial modulation," *IEEE Trans. Veh. Tech.*, vol. 64, no. 6, pp. 2738-2742, Jun. 2015.
- [7] T. Mao, Z. Wang, Q. Wang, S. Chen, and L. Hanzo, "Dual-mode index modulation aided OFDM," *IEEE Access*, vol. 5, pp. 50-60, Feb. 2017.